

Domain Reduction Method for Three-Dimensional Earthquake Modeling in Localized Regions, Part I: Theory

by Jacobo Bielak, Kostas Loukakis, Yoshiaki Hisada, and Chiaki Yoshimura

Abstract This article reports on the development of a modular two-step, finite-element methodology for modeling earthquake ground motion in highly heterogeneous localized regions with large contrasts in wavelengths. We target complex geological structures such as sedimentary basins and ridges that are some distance away from the earthquake source. We overcome the problem of multiple physical scales by subdividing the original problem into two simpler ones. The first is an auxiliary problem that simulates the earthquake source and propagation path effects with a model that encompasses the source and a background structure from which the localized feature has been removed. The second problem models local site effects. Its input is a set of equivalent localized forces derived from the first step. These forces act only within a single layer of elements adjacent to the interface between the exterior region and the geological feature of interest. This enables us to reduce the domain size in the second step. If the background subsurface structure is simple, one can replace the finite-element method in the first step with an alternative efficient method. The methodology is illustrated in a companion paper (Yoshimura *et al.*, 2003) for several 3D problems of increasing physical and computational complexity. We consider first a flat-layered, stratigraphic system. For this simple case, the first step can be carried out by means of 3D Green's function evaluations. The extension to more general problems is illustrated by two examples: a basin and a hill, with the same background stratigraphy. To verify the two-step procedure with a problem for which the finite-element method is used throughout, we model ground motion in a small region of the Los Angeles Basin, using both the two-step domain-reduction method and the traditional approach in which the computational domain contains both the source and the geological region of interest.

Introduction

In the past 10 years tremendous growth has occurred in the development of physics-based 3D models for simulating earthquake ground motion in seismic regions. During this period, numerical modeling methods for anelastic wave propagation that take into consideration the earthquake source, propagation path, and local site effects have become increasingly available. There are several types of such methods. Boundary element and discrete wavenumber methods have been popular for moderate-sized problems with relatively simple geometry and geological conditions (e.g., Mossessian and Dravinski, 1987; Kawase and Aki, 1990; Hisada *et al.*, 1993; Sánchez-Sesma and Luzón, 1995; Bouchon and Barker, 1996). Finite differences (e.g., Frankel and Vidale, 1992; Frankel, 1993; Graves, 1993, 1996; Olsen *et al.*, 1995; Pitarka, 1999; Stidham *et al.*, 1999; Sato *et al.*, 1999) and finite elements (e.g., Lysmer and Drake, 1971; Toshinawa and Ohmachi, 1992; Bao, 1998; Bao *et al.*, 1998; Aagaard *et al.*, 2001) are better suited for larger-sized prob-

lems that involve realistic basin models with highly heterogeneous materials, because of their flexibility and simplicity. Computer codes based on these methods have been used successfully to model earthquake ground motion in a variety of applications; for instance, near-source ground motion (e.g., Wald and Heaton, 1994), basin structure and directivity effects (e.g., Olsen and Archuleta, 1996; Pitarka *et al.*, 1998), and edge effects (e.g., Kawase, 1996; Hisada *et al.*, 1998; Aagaard *et al.*, 2001).

Despite the recent advances in ground-motion simulation capabilities for earthquake excitation (Fig. 1), researchers nowadays are still forced to make restrictive simplifications and approximations in "3D simulations," such as limiting the maximum frequency or lowest wave velocities that can be considered. One reason is that most methods currently in use for large-size problems are based on uniform structured grids. The grid size, which is proportional to the lowest shear wave velocity in the model and inversely pro-

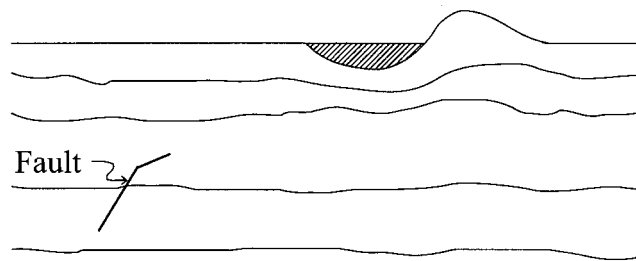


Figure 1. Schematic of semi-infinite seismic region, including causative fault, geological structure and local features.

portional to the highest frequency of interest, is held constant throughout the computational domain even if the softest soils occupy only a small region. Finite-element and other methods with irregular grids (Bao *et al.*, 1998; Pitarka, 1999; Aoi and Fujiwara, 1999; Kristek *et al.*, 1999; Oprsal and Zahradník, 1999, 2002) are more flexible, because they can better tailor the mesh size to the local wavelength of the propagating waves. Regardless of their differences, one feature that is common to traditional finite-difference and finite-element methods is that the ground motions near the causative fault, and those along the propagation path and within the region of interest, are all calculated simultaneously, using a single model that encompasses the whole geological structure, from the fault region to the region of interest. Thus, source, propagation path, and local site effects are determined all at once. This single-pass approach works well for many applications. However, if the source is far from the region of interest, the problem size becomes exceedingly large and the methods become ineffective.

An alternative formulation, which avoids the need to represent accurately the geometric and material properties of the whole region within a single model, consists in subdividing the problem into two sequential parts. First, one considers a background structure from which the localized geological features have been deleted, and calculates the corresponding ground motion. This computation requires a grid or mesh that is only as fine as dictated by the softest material in the background model; it needs to be performed only once for a specified earthquake source. In a second step, only a reduced region of interest which contains the localized feature is modeled to the desired accuracy. The ground motion obtained in the first step is used to determine a set of localized equivalent forces, which are then applied as input over a computational domain that is only slightly bigger than the geologic feature. Only the second part of the computation needs to be repeated if any system parameters within the region of interest need to be varied. Such a two-step procedure was developed by Bielak and his coworkers in the framework of the finite-element method, originally for building–soil–foundation interaction problems (Bielak and Christiano, 1984; Cremonini *et al.*, 1988), and later applied to ground motion modeling of 2D sedimentary valleys in a half-space due to incident plane *SV* waves (Loukakis, 1988;

Loukakis and Bielak, 1994a,b). Similar procedures have been presented by Clough and Penzien (1975), Kausel *et al.* (1978), and Aydinoglu (1980, 1993), under some restrictive assumptions. Other researchers have developed alternative two-step or hybrid procedures that make use of combinations of different computational methods; for example, the wavenumber method and finite differences (Zahradník and Moczo, 1996); modal summation method and finite differences (Regan and Harkrider, 1989; Fäh *et al.*, 1993, 1994); finite-element and boundary integral methods (Mita and Luco, 1987; Bielak *et al.*, 1991); and wavenumber method, finite differences, and finite elements introduced to represent irregular geometries (Moczo *et al.*, 1997). A review of various hybrid methods dating back to 1980 can be found in Moczo *et al.* (1997). All these methods were concerned with 2D applications. An extension of the finite-difference approach to three dimensions has been developed recently by Oprsal and Zahradník (2002).

In this set of two articles we extend the modular two-step procedure developed by Bielak and his co-workers to 3D problems. We use a finite-element formulation in which the primary unknowns are the total wave field within the domain that contains the localized structure and a scattered wave field in the exterior domain. This requires that we store the free-field displacements from the background structure only in a single layer of elements at the interface of the two domains in the first step; it enables us to reduce the size of the computational domain in the second step. This methodology, which we call the domain reduction method (DRM), is capable of efficiently modeling 3D wave fields for an arbitrary earthquake source in highly heterogeneous geological systems with large localized impedance contrasts and arbitrary shapes. To validate this procedure, in a companion article (Yoshimura *et al.*, 2003) we consider a flat-layered system for which a solution can be obtained readily by evaluating the corresponding Green's functions (Hisada, 1994, 1995) and illustrate its applicability to more general problems with two examples, one involving an idealized basin and the other, a hill. To verify the two-step procedure with a problem for which the finite-element method is used in both steps, we model ground motion in a small region of the Los Angeles Basin, using both the two-step DRM, and the traditional approach in which the computational domain contains both the source and the geological region of interest. Whereas the methodology is applicable to elastic, anelastic, and inelastic problems, only the elastic case is considered explicitly in this set of articles for clarity of presentation. In the concluding remarks, however, we discuss briefly the extension to the more general situations. It will be seen that the use of the DRM can be advantageous even in situations in which the causative fault is not far from the region of interest.

Formulation of Domain Reduction Method

We treat the problem of a semi-infinite seismic region that contains localized geological features such as sedimen-

tary valleys and ridges as well as seismically active faults, as shown in Figure 1, under earthquake excitation. The geometry is arbitrary; the material is linearly elastic, and the earthquake excitation is prescribed as a kinematic source along a predetermined fault.

Because the causative fault can be far from the geological features, we wish to define a new problem in which the excitation is brought closer to the region of interest. Such transfer, of course, needs to be performed in a way that the resulting ground motion within the region of interest is identical with that due to the original source. To fix ideas, suppose the new excitation is to be specified on the fictitious surface Γ shown in Figure 2a. This interface divides the seismic region into two parts: Ω , which contains the geological features of interest, and Ω^+ , the semi-infinite exterior subdomain, which includes the fault. We will determine the appropriate expressions for the equivalent excitation using a finite-element formulation. First, the original semi-infinite region needs to be truncated for computational reasons. This is indicated in Figure 2 by the inclusion of the outer boundary Γ^+ . We assume, for the time being, that it is far enough from the fault that no waves reflected from Γ^+ reach Ω within the time under consideration. This assumption will be removed later.

Let the vector field of nodal displacements in the interior domain Ω , the exterior domain Ω^+ , and the boundary between them, Γ , be denoted, respectively, by u_i (interior), u_e (exterior), and u_b (boundary), as shown in Figure 2a. The seismic excitation is prescribed as a kinematic source, defined by the jump of the tangential displacements across the fault; the normal displacements and tractions remain continuous. This excitation can be equivalently specified by means of body forces (e.g., Aki and Richards, 1980). With this representation, a standard application of Galerkin's ideas with finite-element spatial discretization yields a set of nodal

forces, P_e , which act in the vicinity of the fault (e.g., Bao, 1998).

Rather than analyzing simultaneously the entire domain, which includes both the fault and the localized structure, we would like to focus on the response of a smaller region restricted to a neighborhood of the local structure. To this end, we partition the total domain into two separate subdomains as depicted in Figure 2b. One contains the fault and the other the localized geological feature. The displacements u_b are continuous across Γ , and P_b are the nodal forces transmitted by Ω^+ onto Ω .

The ground motion within the entire computational domain is governed by Navier's equations of elastodynamics. When these equations are discretized spatially by finite elements in Ω and Ω^+ , they can be expressed in partitioned form as:

$$\begin{bmatrix} M_{ii}^{\Omega} & M_{ib}^{\Omega} \\ M_{bi}^{\Omega} & M_{bb}^{\Omega} \end{bmatrix} \begin{Bmatrix} \dot{u}_i \\ \dot{u}_b \end{Bmatrix} + \begin{bmatrix} K_{ii}^{\Omega} & K_{ib}^{\Omega} \\ K_{bi}^{\Omega} & K_{bb}^{\Omega} \end{bmatrix} \begin{Bmatrix} u_i \\ u_b \end{Bmatrix} = \begin{Bmatrix} 0 \\ P_b \end{Bmatrix}, \text{ in } \Omega \quad (1)$$

and

$$\begin{bmatrix} M_{bb}^{\Omega^+} & M_{be}^{\Omega^+} \\ M_{eb}^{\Omega^+} & M_{ee}^{\Omega^+} \end{bmatrix} \begin{Bmatrix} \dot{u}_b \\ \dot{u}_e \end{Bmatrix} + \begin{bmatrix} K_{bb}^{\Omega^+} & K_{be}^{\Omega^+} \\ K_{eb}^{\Omega^+} & K_{ee}^{\Omega^+} \end{bmatrix} \begin{Bmatrix} u_b \\ u_e \end{Bmatrix} = \begin{Bmatrix} -P_b \\ P_e \end{Bmatrix}, \text{ in } \Omega^+ \quad (2)$$

In these equations, the matrices M and K denote mass and stiffness matrices, the subscripts i, e, and b refer to nodes in either the interior or the exterior domain or on their common boundary, and the superscripts Ω and Ω^+ refer to the domains over which the various matrices are defined.

The traditional form of the equation of motion for the total domain is obtained by adding (1) and (2):

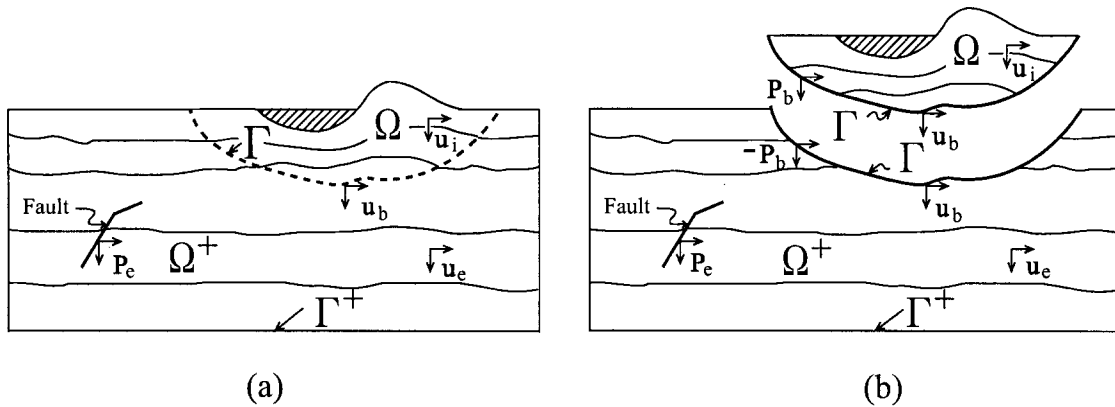


Figure 2. Truncated seismic region. (a) Outer boundary Γ^+ restricts computations to a finite domain; fictitious interface Γ divides region into two subdomains: Ω^+ , which includes the seismic source, represented by nodal forces P_e , and Ω , which contains the localized geological features. (b) Regions partitioned explicitly into two substructures across interface Γ ; P_e are nodal forces transmitted from Ω^+ onto Ω ; $-P_e$ are corresponding reactions from Ω onto Ω^+ ; nodal displacements u_b are required to be continuous across Γ .

$$\begin{bmatrix} M_{ii}^{\Omega} & M_{ib}^{\Omega} & 0 \\ M_{bi}^{\Omega} & M_{bb}^{\Omega} + M_{bb}^{\Omega^+} & M_{be}^{\Omega^+} \\ 0 & M_{eb}^{\Omega^+} & M_{ee}^{\Omega^+} \end{bmatrix} \begin{Bmatrix} \ddot{u}_i \\ \ddot{u}_b \\ \ddot{u}_e \end{Bmatrix} + \begin{bmatrix} K_{ii}^{\Omega} & K_{ib}^{\Omega} & 0 \\ K_{bi}^{\Omega} & K_{bb}^{\Omega} + K_{bb}^{\Omega^+} & K_{be}^{\Omega^+} \\ 0 & K_{eb}^{\Omega^+} & K_{ee}^{\Omega^+} \end{bmatrix} \begin{Bmatrix} u_i \\ u_b \\ u_e \end{Bmatrix} = \begin{Bmatrix} 0 \\ 0 \\ P_e \end{Bmatrix} \quad (3)$$

Now, to transfer the seismic excitation from the fault to Γ , we consider an auxiliary problem in which the exterior region and the material therein, as well as the causative fault, are identical with those of the original problem. The interior domain, now denoted as Ω_0 , is, however, a simpler, background structure, that does not include the localized geological features. This is illustrated in Figure 3a. Ω_0 is chosen such that the new problem defined over the total domain $\Omega_0 \cup \Omega^+$ is easier to solve than the original problem. We denote by u_i^0 , u_b^0 , u_e^0 , and P_b^0 the corresponding nodal displacements and the interface forces, as shown in Figure 3b. The subscripts i, b, and e, have the same meaning as before. After spatial discretization, the equations of motion in Ω^+ for the auxiliary problem can be written as:

$$\begin{bmatrix} M_{bb}^{\Omega^+} & M_{be}^{\Omega^+} \\ M_{eb}^{\Omega^+} & M_{ee}^{\Omega^+} \end{bmatrix} \begin{Bmatrix} \ddot{u}_b^0 \\ \ddot{u}_e^0 \end{Bmatrix} + \begin{bmatrix} K_{bb}^{\Omega^+} & K_{be}^{\Omega^+} \\ K_{eb}^{\Omega^+} & K_{ee}^{\Omega^+} \end{bmatrix} \begin{Bmatrix} u_b^0 \\ u_e^0 \end{Bmatrix} = \begin{Bmatrix} -P_b^0 \\ P_e \end{Bmatrix} \quad (4)$$

The partitioned mass and stiffness matrices, as well as P_e , are the same as in (2) because the material properties in Ω^+ and the earthquake source are identical in both cases.

From the second equation in (4), we can now express the nodal forces P_e in terms of the free field, as follows:

$$P_e = M_{eb}^{\Omega^+} \ddot{u}_b^0 + M_{ee}^{\Omega^+} \ddot{u}_e^0 + K_{eb}^{\Omega^+} u_b^0 + K_{ee}^{\Omega^+} u_e^0 \quad (5)$$

Then, by substituting (5) into (3), we can solve for the displacements u_i , u_b , and u_e for the complete domain. This formulation by itself, however, offers no advantage over the traditional approach because (5) includes the terms

$M_{ee}^{\Omega^+} \ddot{u}_e^0$ and $K_{ee}^{\Omega^+} u_e^0$, which require that the free field u_e^0 be stored throughout the domain Ω^+ . This entails an undue computational effort.

To simplify the analysis, we use a transformation of variables, by which we express the total displacement u_e as the sum of the free field due to the background structure and the residual field due to the localized geological feature:

$$u_e = u_e^0 + w_e \quad (6)$$

That is, the residual field w_e is the relative displacement field with respect to the reference free field u_e^0 .

Then, substituting (6) into (3), and writing the terms that contain the free field on the right side, results in:

$$\begin{bmatrix} M_{ii}^{\Omega} & M_{ib}^{\Omega} & 0 \\ M_{bi}^{\Omega} & M_{bb}^{\Omega} + M_{bb}^{\Omega^+} & M_{be}^{\Omega^+} \\ 0 & M_{eb}^{\Omega^+} & M_{ee}^{\Omega^+} \end{bmatrix} \begin{Bmatrix} \ddot{u}_i \\ \ddot{u}_b \\ \ddot{w}_e \end{Bmatrix} + \begin{bmatrix} K_{ii}^{\Omega} & K_{ib}^{\Omega} & 0 \\ K_{bi}^{\Omega} & K_{bb}^{\Omega} + K_{bb}^{\Omega^+} & K_{be}^{\Omega^+} \\ 0 & K_{eb}^{\Omega^+} & K_{ee}^{\Omega^+} \end{bmatrix} \begin{Bmatrix} u_i \\ u_b \\ w_e \end{Bmatrix} = \begin{Bmatrix} 0 \\ -M_{be}^{\Omega^+} \ddot{u}_e^0 - K_{be}^{\Omega^+} u_e^0 \\ P_e - M_{ee}^{\Omega^+} \ddot{u}_e^0 - K_{ee}^{\Omega^+} u_e^0 \end{Bmatrix} \quad (7)$$

Finally, after substituting for P_e from (5) into (7), we obtain the desired equation:

$$\begin{bmatrix} M_{ii}^{\Omega} & M_{ib}^{\Omega} & 0 \\ M_{bi}^{\Omega} & M_{bb}^{\Omega} + M_{bb}^{\Omega^+} & M_{be}^{\Omega^+} \\ 0 & M_{eb}^{\Omega^+} & M_{ee}^{\Omega^+} \end{bmatrix} \begin{Bmatrix} \ddot{u}_i \\ \ddot{u}_b \\ \ddot{w}_e \end{Bmatrix} + \begin{bmatrix} K_{ii}^{\Omega} & K_{ib}^{\Omega} & 0 \\ K_{bi}^{\Omega} & K_{bb}^{\Omega} + K_{bb}^{\Omega^+} & K_{be}^{\Omega^+} \\ 0 & K_{eb}^{\Omega^+} & K_{ee}^{\Omega^+} \end{bmatrix} \begin{Bmatrix} u_i \\ u_b \\ w_e \end{Bmatrix} = \begin{Bmatrix} 0 \\ -M_{be}^{\Omega^+} \ddot{u}_e^0 - K_{be}^{\Omega^+} u_e^0 \\ M_{eb}^{\Omega^+} \ddot{u}_b^0 + K_{eb}^{\Omega^+} u_b^0 \end{Bmatrix} \quad (8)$$

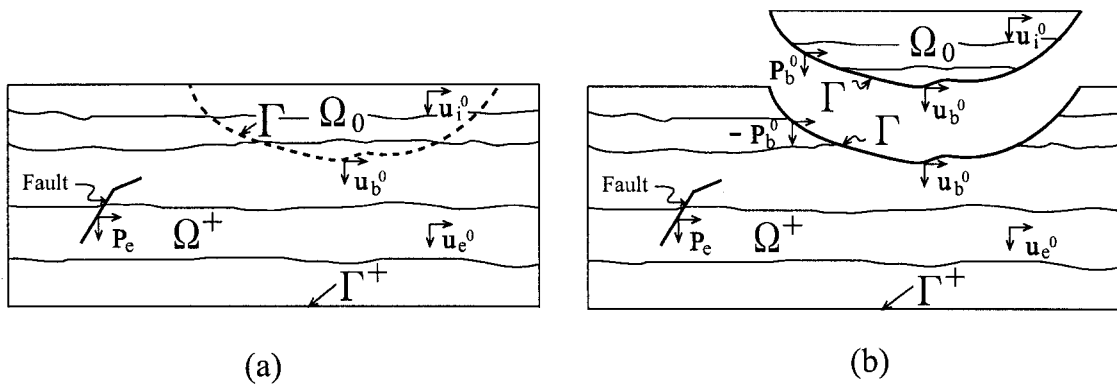


Figure 3. Auxiliary seismic region. Localized geological features of actual problem in Ω have been replaced by a simpler background structure over domain Ω_0 . (a) Entire region; (b) region partitioned into two substructures.

The mass matrix and stiffness matrix in the left hand side of (8) are identical with those of (3). However, the seismic forces P_e on the fault have been replaced by the effective nodal forces P^{eff} , given by:

$$P^{eff} = \begin{Bmatrix} P_i^{eff} \\ P_b^{eff} \\ P_e^{eff} \end{Bmatrix} = \begin{Bmatrix} 0 \\ -M_{bc}^{\Omega^+} \ddot{u}_c^0 - K_{bc}^{\Omega^+} u_c^0 \\ M_{cb}^{\Omega^+} \ddot{u}_b^0 + K_{cb}^{\Omega^+} u_b^0 \end{Bmatrix} \quad (9)$$

These forces have the key property that they involve only the submatrices M_{bc} , K_{bc} , M_{cb} , and K_{cb} , which vanish everywhere except in a single layer of finite elements in Ω^+ adjacent to Γ . This small domain lies between Γ and its adjacent surface Γ_e , as shown in Figure 4. Therefore, the forces P^{eff} act exclusively within that layer. Also, the only wave field needed to determine P^{eff} is that obtained from the auxiliary problem at the nodes that lie on Γ , Γ_e , and between these surfaces. This localization of the equivalent seismic forces around the geologic feature is the key advantage of the transformation (6).

Another important consequence of (9) is that all the waves in the exterior region Ω^+ will be outgoing. This suggests that for solving (8), the size of the region Ω^+ can be drastically reduced if one is interested only in the ground motion near the localized features, provided suitable absorbing boundaries are used to limit the occurrence of spurious waves. Because of this attractive feature, we name our method Domain Reduction Method (DRM). To emphasize this reduction in size, we will denote the reduced exterior region by $\hat{\Omega}^+$ and its corresponding outer boundary by $\hat{\Gamma}^+$. These results were derived originally in the context of a half-space and plane wave excitation in a slightly different form (Bielak and Christiano, 1984; Loukakis, 1988; Loukakis and Bielak, 1994a). The present derivation is more rigorous and concise, and it incorporates explicitly the effect of an extended source on a finite fault. A procedure similar to that in Loukakis (1988) was developed subsequently by Aydinoglu (1993), in the context of soil-structure interaction without explicit treatment of the earthquake source. Instead of using a finite-element formulation throughout as in Loukakis (1988) and Loukakis and Bielak (1994a), Aydinoglu (1993) used a boundary integral representation for the tractions at the interface between the interior and exterior domains; to make the equations local at the interface, the traction was approximated in the form of a mass-dashpot-spring, and the material outside the interface Γ was excluded from the computations. It is not clear that this simplification will lead to acceptable approximations. In addition, contrary to our formulation, in which the effective forces depend only on the properties of the material within the region exterior to Ω , the effective forces are defined on a layer within the interior region. This could pose some difficulty if one is interested in considering interior regions that behave nonlinearly, as discussed in the next section. Similar results were derived also by Zahradnik and Moczo (1996) for the finite difference method in two dimensions using a rectangular

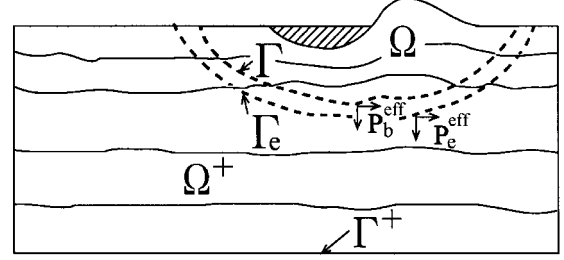


Figure 4. Seismic region with two neighboring surfaces Γ and Γ_e on which effective nodal forces P^{eff} defined by equation (9) are to be applied. These forces are equivalent to and replace the original seismic forces P_e , which act in the vicinity of the causative fault.

excitation box, and an algorithm similar to that of Alterman and Karal (1968) to do the coupling.

Discussion and Concluding Remarks

The results described in the previous paragraphs can be summarized as a two-step procedure for analyzing the earthquake response of localized geological features, as follows. In step I, as shown in Figure 5a, one starts with a background geological model that is defined over the domains Ω^+ and Ω_0 , which include the original earthquake source, and that defines the boundary Γ of what will be the region of interest in step II. Then one calculates the free-field ground motion u_b^0 and u_c^0 and stores it at all the nodes on the adjacent surfaces Γ and Γ_e as well as at any interior nodes within the finite element layer that lies between them. Suitable absorbing boundary conditions on Γ^+ , such as those proposed by Clayton and Engquist (1977) and Stacey (1988), must be used to keep spurious wave reflections within acceptable limits. Spurious reflections from the absorbing boundaries are generally unavoidable in practice, and can lead to inaccuracies in the numerical results.

If desired, any appropriate method can be used in step I to determine these wave fields in place of the finite-element method. The second step is performed on a reduced region $\Omega \cup \hat{\Omega}^+$, which contains the geological features of interest, but not the causative fault, as shown in Figure 5b. The effective seismic forces P^{eff} are evaluated first, from (9), using u_b^0 and u_c^0 as input. Once these forces have been established, the total wave fields u_i and u_b , and the residual wave field w_e , defined respectively over Ω , Γ , and $\hat{\Omega}^+$, are obtained by solving (8). Actually, this equation must be modified slightly to incorporate the absorbing boundary conditions on $\hat{\Gamma}^+$. The complete solution u_e within the domain $\hat{\Omega}^+$ can be evaluated simply as $u_e = w_e + u_e^0$.

It is important to emphasize that the DRM is exact to within finite element spatial and time discretization errors. In our implementation we have used piecewise linear finite elements in space, and second-order central differences in time. Thus, our results are second-order accurate in space

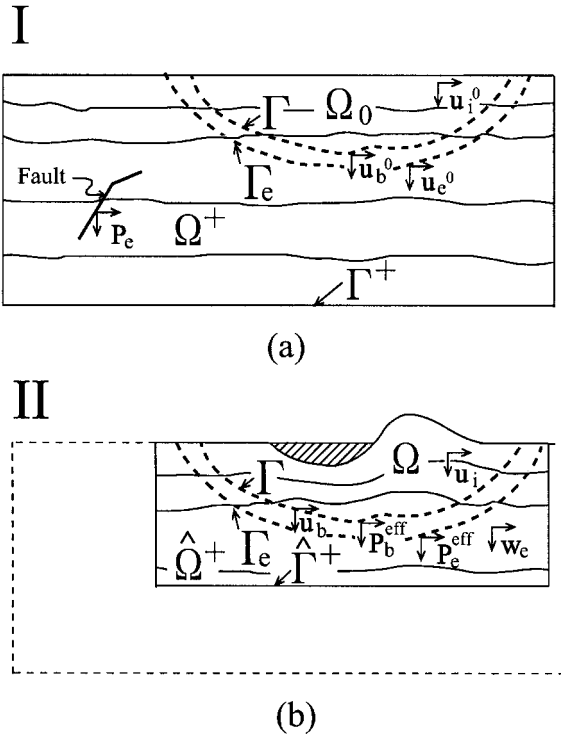


Figure 5. Summary of two-step DRM. (a) Step I defines the auxiliary problem over background geological model. Resulting nodal displacements within Γ , Γ_e , and the region between them are used to evaluate effective seismic forces P^{eff} required for step II. (b) Step II, defined over reduced region made up of Ω and $\hat{\Omega}^+$ (a truncated portion of Ω^+). The effective seismic forces P^{eff} are applied within Γ and Γ_e . The unknowns are the total displacement fields u_i in Ω and u_b on Γ , and the residual displacements w_c in $\hat{\Omega}^+$.

and time. The main computational efficiency is gained from the use of the finite-element method, which allows one to tailor the mesh size to the local wavelength of the propagating wave, and to the reduction of the overall computational domain in the second step, which might be quite dramatic if the source is far, the material within the region of interest is nonlinear, or repeated solutions with minor changes in the parameters are required, as in inverse problems. With the goal of increasing the computational efficiency of 3D simulations, other authors have developed powerful memory optimization methods, especially in the context of the finite-difference method, to be able to deal with more realistic material properties and frequencies closer to those of engineering interest. In particular, Moczo *et al.* (1999) use a lossy compression scheme based on a discrete wavelet transform to optimize RAM and disk storage requirements. Combining the compression scheme with the memory optimization of Graves (1996) and the memory variable economization of Day (1998) and Day and Bradley (2001), Moczo *et al.* (2000, 2001) in some cases achieve a total disk plus RAM storage reduction approaching or exceeding an order of magnitude. Such optimization tech-

niques could be applied also to the DRM to attain further storage reductions.

It should also be emphasized that the strict validity of our two-step methodology hinges on the linearity of the material outside the region of interest Ω and on the requirement that the material properties in the exterior region be the same for the auxiliary problem as for the original problem. The material within Ω , on the other hand, can be arbitrary. Notice that its properties do not enter into the computation of P^{eff} . In fact, the two-step procedure we just described would remain valid even if the material in Ω were nonlinear. All that would change in the formulation are the stiffness terms in (3) and (7) pertaining to the interior domain, which would then depend on the solution. More generally, the second term in (1) and in subsequent equations would be a nonlinear function of u_i and u_b , which would depend on the material constitutive equations. Another assumption in our derivation is that the material is nondissipative. Clearly, adding linear dissipation would not change the essence of the procedure, but merely modify the particular form of the equations. For instance, the addition of viscous damping would result in added terms proportional to velocity in the equations (Loukakis, 1988; Loukakis and Bielak, 1994b). More generally, linear viscoelastic behavior would, rigorously, introduce convolutions into the semidiscretized formulation. Such convolutions, however, can be avoided if one approximates the viscoelastic dependence by a linear combination of multiple relaxation mechanisms that can be expressed in differential form with the aid of auxiliary memory variables (e.g., Day and Minster, 1984; Emmerich and Korn, 1987; Carcione *et al.* 1988; Moczo *et al.*, 1997). One important drawback encountered originally with these methods was the added computational and storage cost associated with the auxiliary memory variables. This difficulty has been partially removed by the coarse-graining methodology developed by Day (1998), in which only one individual relation mechanism per node produces highly accurate results.

Acknowledgments

This work was supported by the National Science Foundation, under grant CMS-9980063 of the KDI program, and under grant EEC-0121989 of the Engineering Research Centers. The cognizant program directors are Clifford J. Astill and Joy M. Pauschke, respectively. This work was also partly supported by a special project of U.S.–Japan Cooperative Research for Urban Earthquake Disaster Mitigation (11209201), Grant-in-Aid for Scientific Research on Priority Area (Category B), Ministry of Education, Culture, Sports, Science, and Technology of Japan (PI: Tomotaka Iwata), and by Taisei Corporation. We are grateful for this support. We thank Peter Moczo and an anonymous reviewer, whose reviews helped us improve the manuscript. The work was done while one of the authors (C. Y.) was visiting Carnegie Mellon University as a research scholar on leave from Taisei Corporation.

References

- Aagaard, B. T., J. F. Hall, and T. Heaton (2001). Characterization of near-source ground motions with earthquake simulations, *Earthquake Spectra* **17**, 177–207.

- Aki, K., and P. G. Richards (1980). *Quantitative Seismology: Theory and Methods*, W. H. Freeman, New York.
- Alterman, Z., and F. C. Karal, Jr. (1968). Propagation of elastic waves in layered media by finite difference methods, *Bull. Seism. Soc. Am.* **58**, 367–398.
- Aoi, S., and H. Fujiwara (1999). 3-D finite difference method using discontinuous grids, *Bull. Seism. Soc. Am.* **89**, 918–930.
- Aydinoğlu, M. N. (1980). Unified formulations for soil-structure interaction, in *Proc. 7th World Conf. Earthquake Engineering*, Istanbul, Turkey, 8–13 September 1980, Vol. 7, 121–128.
- Aydinoğlu, M. N. (1993). Consistent formulation of direct and substructure methods in nonlinear soil-structure interaction, *Soil Dyn. Earthquake Eng.* **12**, 403–410.
- Bao, H. (1998). Finite element simulation of earthquake ground motion in realistic basins, *Ph.D. Thesis*, Carnegie Mellon University, Pittsburgh.
- Bao, H., J. Bielak, O. Ghattas, L. F. Kallivokas, D. R. O'Hallaron, J. R. Shewchuk, and J. Xu (1998). Large-scale simulation of elastic wave propagation in heterogeneous media on parallel computers, *Comput. Methods Appl. Mech. Eng.* **152**, 85–102.
- Bielak, J., and P. Christiano (1984). On the effective seismic input for nonlinear soil-structure interaction systems, *Earthquake Eng. Struct. Dyn.* **12**, 107–119.
- Bielak, J., R. C. MacCamy, D. S. McGhee, and A. Barry (1991). Unified symmetric BEM-FEM for site effects on ground motion—SH waves, *J. Eng. Mech.* **117**, 2265–2285.
- Bouchon, M., and J. S. Barker (1996). Seismic response of a hill: The example of Tarzana, California, *Bull. Seism. Soc. Am.* **86**, 66–72.
- Carcione, J. M., D. Kosloff, and R. Kosloff (1988). Wave propagation in a linear viscoacoustic medium, *J. R. Astr. Soc.* **78**, 105–118.
- Clayton, R. W., and B. Engquist (1977). Absorbing boundary conditions for acoustic and elastic wave equations, *Bull. Seism. Soc. Am.* **67**, 1529–1540.
- Clough, R. W., and J. Penzien (1975). *Dynamics of Structures*, McGraw-Hill, New York, 584.
- Cremonini, M. G., P. Christiano, and J. Bielak (1988). Implementation of effective seismic input for soil-structure interaction systems, *Earthquake Eng. Struct. Dyn.* **16**, 615–625.
- Day, S. M. (1988). Efficient simulation of constant Q using coarse-grained memory variables, *Bull. Seism. Soc. Am.* **88**, 105–1062.
- Day, S. M., and C. R. Bradley (2001). Memory-efficient simulation of anelastic wave propagation, *Bull. Seism. Soc. Am.* **91**, 520–531.
- Day, S. M., and J. B. Minster (1984). Numerical simulation of attenuated wavefields using a Padé approximant method, *Geophys. J. R. Astr. Soc.* **78**, 105–118.
- Emmerich, H., and M. Korn (1987). Incorporation of attenuation into time domain computations of seismic wave fields, *Geophysics* **52**, 1252–1264.
- Fäh, D., P. Suhadolc, and G. F. Panza (1993). Variability of seismic ground motion in complex media: the case of a sedimentary basin in the Friuli (Italy) area, *J. Appl. Geophys.* **30**, 131–148.
- Fäh, D., P. Suhadolc, St. Mueller, and G. F. Panza (1994). A hybrid method for the estimation of ground motion in sedimentary basins: Quantitative modeling for Mexico City, *Bull. Seism. Soc. Am.* **84**, 383–399.
- Frankel, A., and J. E. Vidale (1992). A three-dimensional simulation of seismic waves in the Santa Clara Valley, California from a Loma Prieta aftershock, *Bull. Seism. Soc. Am.* **82**, 2045–2074.
- Frankel, A. (1993). Three-dimensional simulations of ground motions in the San Bernardino Valley, California, for hypothetical earthquakes on the San Andreas fault, *Bull. Seism. Soc. Am.* **83**, 1024–1041.
- Graves, R. W. (1993). Modeling three-dimensional site response effects in the Marina District Basin, San Francisco, California, *Bull. Seism. Soc. Am.* **83**, 1042–1063.
- Graves, R. W. (1996). Simulating seismic wave propagation in 3D elastic media using staggered-grid finite-differences, *Bull. Seism. Soc. Am.* **86**, 1091–1106.
- Hisada, Y. (1994). An efficient method for computing Green's function for a layered half-space with sources and receivers at close depths, *Bull. Seism. Soc. Am.* **84**, 1456–1472.
- Hisada, Y. (1995). An efficient method for computing Green's function for a layered half-space with sources and receivers at close depths (Part 2), *Bull. Seism. Soc. Am.* **85**, 1080–1093.
- Hisada, Y., K. Aki, and T. L. Teng (1993). 3-D simulations of surface wave propagation in the Kanto sedimentary basin, Japan. Part 2: Application of the surface wave BEM, *Bull. Seism. Soc. Am.* **83**, 1700–1720.
- Hisada, Y., H. Bao, J. Bielak, O. Gattas, and D. R. O'Hallaron (1998). Simulation of long-period ground motions during the 1995 Hyogo-ken-Nanbu (Kobe) earthquake using 3-D finite element method, in *Proc. 2nd International Symposium on the Effect of Surface Geology on Seismic Motion*, 1–3 December 1998, Yokohama, Japan, 1353–1360.
- Kausel, E., R. V. Whitman, J. P. Murray, and F. Elsabee (1978). The spring method for embedded foundations, *Nucl. Eng. Des.* **48**, 377–392.
- Kawase, H. (1996). The cause of the damage belt in Kobe: “the basin-edge effect”, constructive interference of the direct S-wave with the basin-induced diffracted/Rayleigh wave, *Seism. Res. Lett.* **67**, 25–34.
- Kawase, H., and K. Aki (1990). Topography effect at the critical SV-wave incidence: Possible explanation of damage pattern by the Whittier Narrows, California, earthquake of 1 October 1987, *Bull. Seism. Soc. Am.* **80**, 1–22.
- Kristek, J., P. Moczo, K. Irikura, T. Iwata, and H. Sekiguchi (1999). The 1995 Kobe mainshock simulated by the 3D finite differences, in *The Effects of Surface Geology on Seismic Motion*, K. Irikura, et al. (Editors), Vol. 3, Balkema, Rotterdam, 1361–1368.
- Loukakis, K. E. (1988). Transient response of shallow layered valleys for inclined incident SV waves calculated by the finite element method, *M.Sc. Thesis*, Carnegie Mellon University, Pittsburgh.
- Loukakis, K., and J. Bielak (1994a). Seismic response of two-dimensional sediment-filled valleys to oblique incident SV-waves calculated by the finite element method, in *Proceeding of the Fifth U.S. National Conference on Earthquake Engineering*, 10–14 July 1994, Chicago, Illinois, Vol. III, 25–34.
- Loukakis, K., and J. Bielak (1994b). Layering and damping effects on seismic response of sedimentary valleys to oblique excitation, in *Proceedings of the Second International Conference on Earthquake Resistant Construction and Design*, 15–17 June 1994, Berlin, Germany, 93–100.
- Lysmer, J., and L. A. Drake (1971). The propagation of Love waves across nonhorizontally layered structures, *Bull. Seism. Soc. Am.* **61**, 1233–1252.
- Mita, A., and J. E. Luco (1987). Dynamic response of embedded foundations: a hybrid approach, *Comput. Methods Appl. Mech. Eng.* **63**, 233–259.
- Moczo, P., E. Bystrický, J. Kristek, J. M. Carcione, and M. Bouchon (1997). Hybrid modeling of P-SV seismic motion at inhomogeneous viscoelastic topographic structures, *Bull. Seism. Soc. Am.* **87**, 1305–1323.
- Moczo, P., J. Kristek, and E. Bystrický (2001). Efficiency and optimization of the 3D finite-difference modeling of seismic ground motion, *J. Comput. Acoust.* **9**, 593–609.
- Moczo, P., M. Lucká, J. Kristek, and M. Kristeková (1999). 3D displacement finite differences and a combined memory optimization, *Bull. Seism. Soc. Am.* **89**, 69–79.
- Mossessian, T., and M. Dravinski (1987). Application of a hybrid method for scattering of P, SV, and Rayleigh waves by near-surface irregularities, *Bull. Seism. Soc. Am.* **77**, 1784–1803.
- Olsen K. B., J. C. Pechmann, and G. T. Schuster (1995). Simulation of 3D elastic wave propagation in the Salt Lake basin, *Bull. Seism. Soc. Am.* **85**, 1688–1710.
- Olsen K. B., and R. J. Archuleta (1996). 3D simulation of earthquakes on the Los Angeles fault system, *Bull. Seism. Soc. Am.*, **86**, 575–596.
- Oprsal, I., and J. Zahradník (1999). Elastic finite-difference method for irregular grids, *Geophysics* **64**, 240–250.
- Oprsal, I., and J. Zahradník (2002). Three-dimensional finite difference

- method and hybrid modeling of earthquake ground motion, *J. Geophys. Res.* **107** (B8), 2161, doi:10.1029/2000JB000082.
- Pitarka A. (1999). 3D elastic finite-difference modeling of seismic motion using staggered grids with non-uniform spacing, *Bull. Seism. Soc. Am.* **89**, 54–68.
- Pitarka, A., K. Irikura, T. Iwata, and H. Sekiguchi (1998). Three-dimensional simulation of the near-fault ground motion for the 1995 Hyogoken Nanbu (Kobe), Japan, earthquake, *Bull. Seism. Soc. Am.* **88**, 428–440.
- Regan, J., and D. G. Harkrider (1989). Numerical modelling of SH L_g waves in and near continental margins, *Geophys. J. Int.* **98**, 107–130.
- Sánchez-Sesma, F. J., and F. Luzón (1995). Seismic response of three-dimensional valleys for incident P, S, and Rayleigh waves, *Bull. Seism. Soc. Am.* **85**, 269–284.
- Sato, T., R. W. Graves, and P. G. Somerville (1999). Three-dimensional finite-difference simulations of long-period strong motions in the Tokyo metropolitan area during the 1990 Odawara earthquake (M_J 5.1) and the great 1923 Kanto earthquake (M_S 8.2) in Japan, *Bull. Seism. Soc. Am.* **89**, 579–607.
- Stacey, R. (1988). Improved transparent boundary formulations for the elastic-wave equation, Short Note, *Bull. Seism. Soc. Am.* **78**, 2089–2097.
- Stidham, C., M. Antolik, D. Dreger, S. Larsen, and B. Romanowicz (1999). Three-dimensional structure influences on the strong motion wavefield of the 1989 Loma Prieta earthquake, *Bull. Seism. Soc. Am.* **89**, 1184–1202.
- Toshinawa, T., and T. Ohmachi (1992). Love wave propagation in a three-dimensional sedimentary basin, *Bull. Seism. Soc. Am.* **82**, 1661–1667.
- Wald, D. J., and T. H. Heaton (1994). Spatial and temporal distribution of slip for the 1992 Landers, California, earthquake, *Bull. Seism. Soc. Am.* **84**, 668–691.
- Yoshimura, C., J. Bielak, Y. Hisada, and A. Fernández (2002). Domain reduction method for three-dimensional earthquake modeling in localized regions, Part II: Verification and applications, *Bull. Seism. Soc. Am.* **93**, no. 2, 825–840.
- Zahradník, J. (1995). Simple elastic finite-difference scheme, *Bull. Seism. Soc. Am.* **85**, 1879–1887.
- Zahradník, J., and P. Moczo (1996). Hybrid seismic modeling based on discrete-wavenumber and finite-difference methods, *Pure Appl. Geophys.* **148**, 21–38.

Department of Civil and Environmental Engineering
Carnegie Mellon University
Pittsburgh, PA 15213-3890
jbielak@cmu.edu
(J.B.)

Technical Company of General Construction
Isiodou 22, Athens 10674, Greece
kloukakis@compulink.gr
(K.L.)

Department of Architecture
Kogakuin University
1-24-2 Nishi-shinjuku, Shinjuku-ku
Tokyo 163-8677, Japan
hisada@cc.kogakuin.ac.jp
(Y.H.)

Technology Center
Taisei Corporation
344-1 Nase-cho, Totsuka-ku
Yokohama 245-0051, Japan
yosimura@eng.taisei.co.jp
(C.Y.)

Manuscript received 21 September 2001.